12 Annual Conference of the Materials Research Society of Serbia, Herceg Novi, Montenegro, September 6–10, 2010

Binding Energy of the Hydrogenic Impurity in CdTe/ZnTe Spherical Quantum Dot

D. Stojanović*, R. Kostić

University of Belgrade, Institute of Physics, P.O. Box 68, 11080 Belgrade, Serbia

Binding energy of a hydrogenic impurity located at the center of the CdTe/ZnTe spherical quantum dot has been calculated under the effective mass approximation by solving Schrödinger equation analytically. Eigen energies are expressed in terms of the Whittaker function and Coulomb wave function. The results show that impurity binding energy strongly depends on QD size if it is around one effective Bohr radius.

PACS: 73.21.La, 71.55.–i

1. Introduction

Among semiconductor quantum nanostructures serious attention is focused on the zero-dimensional quantum dot (QD). These structures have found various application areas especially as electronic, optoelectronic devices or in bioscience for biolabeling. Therefore, semiconductor QDs, especially their optical properties, have been intensively studied both theoretically and experimentally in applied physics [1].

The electronic states are very sensitive to the dimension of QD. Properties of the materials we combine to form the structure as: confining potential or effective masses of free carriers in materials, can become important for the properties of designed structure. As number of electrons increase, the electron-electron interaction becomes remarkable, the effective potential is changed and the energy levels are pushed up. In presence of the hydrogenic impurity, located inside low-dimensional system as QD, electronic levels are pulled down. Consequently, the electronical and optical properties of these structures can be drastically changed.

Influence of hydrogenic impurity in a low-dimensional system can be experimentally registered and calculated as change in the electronic and optical properties as: donor binding energy, behavior in electric and magnetic field, photoionization cross section, absorption spectra and other optical properties [2].

In last few years CdTe/ZnTe system is under intensive investigation especially as a candidate for spin transfer [3–5]. All parameters of these materials are well established.

The aim of this paper is to present results of calculation of one-electron system with a hydrogenic impurity in the centrum of QD (D^0) i.e. binding energy of the D^0 for particular case of spherical CdTe core surrounded by ZnTe.

* corresponding author; e-mail: dusanka@ipb.ac.rs

2. Theory

The D^0 centre in semiconductor spherical quantum dot can be described as a system composed of an electron and a positively charged donor impurity located at the centre of the spherical potential well region. A single quantum dot embedded in a matrix material is considered. The validity of the effective mass approximation is assumed. Difference of the electron effective masses [6–9] and dielectric constants [10] between the QD region and the surrounding medium are considered.

Considering that electron spectra is mainly formed by size quantization, the stationary Schrödinger equation for D^0 in the approximation of the effective mass has the form

$$\left(-\frac{\hbar^2}{2}\nabla\frac{1}{m^*(r)}\nabla + W(r) + U(r)\right)\Psi(r) = E\Psi(r). \quad (1)$$

where

$$m^*(r) = \begin{cases} m_1^* & r < r_0, \\ m_2^* & r \geq r_0 \end{cases}. \quad (2)$$

is the effective mass of an electron of the heterosystem. In this case m_1^* is effective mass of CdTe, m_2^* is effective mass of ZnTe, Table [11].

The potential energy of interaction of an electron with ion which is located at the center of QD has the form [10]

$$W(r) = -Z\,\mathrm{e}^2 \begin{cases} \frac{\varepsilon_1-\varepsilon_2}{\varepsilon_1\varepsilon_2 r_0} + \frac{1}{\varepsilon_1 r} & r < r_0, \\ \frac{1}{\varepsilon_2 r} & r \geq r_0 \end{cases}. \quad (3)$$

The confinement potential is given as

$$U(r) = \begin{cases} -U_1, & r < r_0, \\ 0 & r \geq r_0 \end{cases} \quad U_1 > 0\,. \quad (4)$$

We assigned a potential energy of zero outside CdTe core. U_1 is barrier height of 670 meV for the electron [12, 13, 14], ε_i are the corresponding static dielectric constant, Table.

Scheme of the potential energy at $r_0 = 3.76$ nm is presented in Fig. 1.

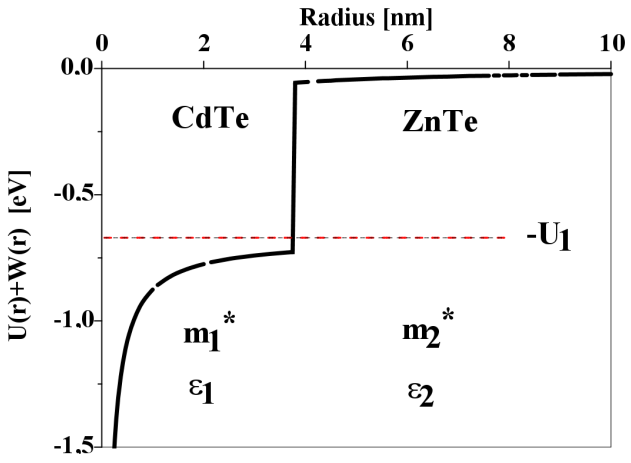

Fig. 1. Potential energy $U(r)+W(r)$ at $r_0=1$, $a_{\rm B}^*=3.76$ nm.

For spherically symmetric potential $U(r)$ the separation of radial and angular coordinates leads to:

$$\Psi_{lm}(r)=R_l(r)Y_{lm}(\theta,\varphi). \tag{5}$$

$R_l(r)$ is the radial wave function, and $Y_{lm}(\theta,\phi)$ is a spherical harmonic. The differential equation for the radial function $R_l(r)$ can be written as

$$-\frac{\hbar^2}{2m^*(r)}\left(\frac{\partial^2}{\partial r^2}+\frac{2}{r}\frac{\partial}{\partial r}-\frac{l(l+1)}{r^2}\right)R_l(r) +(W(r)+U(r))R_l(r)=ER_l(r). \tag{6}$$

The radial function $R_l(r)$, consist of two parts, because it spreads through two different regions:

$$R_l=\begin{cases} R_l^1 & r< r_0 \\ R_l^2 & r\geq r_0 \end{cases}. \tag{7}$$

Solutions must satisfy conditions $R_l(r)$ to be regular when $r=0$ and to vanish sufficiently rapidly when $r\to\infty$.

For $r<r_0$ and energy range $0>E>U_0$, introducing $\alpha_{1b}^2=2m_1(E+U_0)/\hbar^2>0$, $\xi=\alpha_{1b}r$, $\beta_1=m_1e^2/\varepsilon_1\hbar^2\alpha_{1b}$, and $R(\xi)=\xi^{-1}F(\xi)$, where

$$U_0=Z\,\mathrm{e}^2\frac{\varepsilon_1-\varepsilon_2}{\varepsilon_1\varepsilon_2 r_0}+U_1 \quad Z=1\ . \tag{8}$$

Equation (6) becomes

$$\frac{\partial^2F}{\partial\xi^2}+\left[1-\frac{2\beta_1}{\xi}-\frac{l(l+1)}{\xi^2}\right]F=0. \tag{9}$$

Equation (9) is the Coulomb equation which have two linearly independent solutions $F_{\beta_1,l}(\xi)$ and $G_{\beta_1,l}(\xi)$. $G_{\beta_1,l}(\xi)$ is a singular at $\xi=0$, hence the wave function of the radial part is expressed as

$$R_l^1(\alpha_{1b}r)=C_{1b}\sum_{k=l+1}^{\infty}A_k^l(\beta_1)(\alpha_{1b}r)^{k-1}. \tag{10}$$

C_{1b} is the normalization constant [6].

The recurrence relation can be expressed as [6, 15]

$$A_{l+1}^l(\beta_1)=1, \tag{11}$$

$$A_{l+2}^l(\beta_1)=\beta_1/(l+1), \tag{12}$$

$$A_k^l(\beta_1)=\frac{2\beta_1A_{k-1}^l(\beta_1)-A_{k-2}^l(\beta_1)}{(k+l)(k-l-1)}. \tag{13}$$

For energy range $E<-U_0$, where $\alpha_{1a}^2=-8m_1(E+U_0)/\hbar^2$, $\xi=\alpha_{1a}r$, $\lambda_1=2m_1e2/\varepsilon_1\hbar^2\alpha_{1a}$, and $R(\xi)=\xi^{-1}\chi(\xi)$, the radial Schrödinger equation becomes

$$\frac{\partial^2\chi}{\partial\xi^2}+\left[-\frac{1}{4}+\frac{\lambda_1}{\xi}+\frac{\frac{1}{4}-(l+\frac{1}{2})^2}{\xi^2}\right]\chi=0. \tag{14}$$

Equation (14) is the Whittaker equation with two linearly independent solutions. As the wave function has to be finite everywhere, the solution of the radial part is

$$R_l^1(\alpha_{1a}r)=C_{1a}\frac{1}{\xi}M(\lambda_1,l+\frac{1}{2},\alpha_{1a}r). \tag{15}$$

C_{1a} is the normalization constant.

For $r>r_0$, introducing $\alpha_2^2=-8m_2E/\hbar^2$, $\xi=\alpha_2r$, $\lambda_2=2m_2e^2/\varepsilon_2\hbar^2\alpha_2$, and $R(\xi)=\xi-1W(\xi)$, the radial Schrödinger equation becomes the Whittaker equation with two linearly independent solutions. As the wave function has to be finite everywhere, the solution of the radial part is

$$R_l^2(\alpha_2r)=C_2\frac{1}{\xi}W(\lambda_2,l+\frac{1}{2},\alpha_2r). \tag{16}$$

C_2 is the normalization constant, M and W are Whittaker functions.

The solution must satisfy boundary conditions:

$$R_l^1(r)\,|_{r=r_0}=R_l^2(r)\,|_{r=r_0}$$

$$\frac{1}{m_1^*}\frac{dR_l^1(r)}{dr}\,|_{r=r_0}=\frac{1}{m_2^*}\frac{\mathrm{d}R_l^2(r)}{\mathrm{d}r}\,|_{r=r_0}\ . \tag{17}$$

Equations (17) lead to a system of two linear equations for the two unknown normalization constants. It has nontrivial solutions only if its determinant

$$D_l=D_l(E_{nl})=0. \tag{18}$$

Once the eigenvalues E_{nl} are determined from (18), the linear equations can be solved yielding the coefficients to be a function of one of them (n is solution number). The last undetermined coefficient is determined by the normalization condition. As all solutions are determined, we can unify them to get the complete picture of eigensolutions E_{nl} and corresponding wave functions R_{nl}. These calculations were performed for electrons, giving the confinement energies E_{nl} and wave functions R_{nl}. Once the electron wave functions are known, radial probability in the system can give an illustrative picture of electron spatial localization. By analogy to hydrogenic like atom ground state, energy E_{10} ($l=0$, $n=1$) in our notation, can be assigned as $1s$ and the first excited state, energy E_{11} ($l=1$, $n=1$) in our notation, corresponds to $2p$.

The binding energy E_b of a donor impurity is defined as the difference between the energy state of the system without impurity ($Z=0$), and the energy of the corresponding state of the system with impurity ($Z=1$), i.e.,

$$E_b(D^0) = E_0 - E(D^0). \quad (19)$$

E_0 is a electron state energy for QD without impurity and $E(\mathrm{D}^0)$ is corresponding energy state for QD with impurity.

3. Results

We determined ground ($1s$) and excited states ($2p$) energies using above analyses and parameters of CdTe and ZnTe bulk materials. We used exact solution of Poisson equation an take into account the difference between dielectric permittivities of QD and the matrix [10].

TABLE

Material parameters of the system: a — lattice constant, E_g — energy gap, V_e — conduction band offset potential, m_e — electron mass

	a(Å)	E_g (eV)	V_e (eV)	m_e^*/m_e	ε_∞
CdTe	6.478	1.5		0.0999	7.1
ZnTe	6.103	2.27	0.67	0.116	6.7

The effective Rydberg $R_y^* = m_1^* e^4/2h^2\varepsilon_1^2$ is the unit of the energy, the Bohr radius '$a_{\mathrm{B}}^* = h^2\varepsilon_1/m_1^* e^2$ is the unit of the length. For our case 1 $R_y^* \approx 26.96$ meV and 1 $a_{\mathrm{B}}^* \approx 3.76$ nm.

Figure 2 presents the ground ($1s$) and the first excited ($2p$) one-electron QD energy states without ($Z = 0$) and with the impurity ($Z = 1$, i.e. D^0), as a function of dot radius. As seen from the Fig. 2, for $Z = 0$ both energies decrease with dot radius increase and approach asymptotically constant values. For CdTe/ZnTe, case, $1s$ bound level appears at $r \approx 0.3a_{\mathrm{B}}^*$ and $2p$ bound level appears at $r \approx 0.65a_{\mathrm{B}}^*$.

In D^0 ($Z = 1$) corresponding $1s$ and $2p$ energy levels are below $Z = 0$ values. In this case $1s$ bound level appears at $r \approx 0.05a_{\mathrm{B}}^*$ and $2p$ bound level appears at $r \approx 0.4a_{\mathrm{B}}^*$. As the dot radius increase $1s$ energy decreases, goes below $-U_1$, reaches minimum at $r_{\min} \approx 5a_{\mathrm{B}}^*$, insert in Fig. 2, and then slowly increases. For dot radius large compared to $r_{\min}$ the energy asymptotically approaches characteristic value $-U_1 - R_y^*$. As the dot radius increase $2p$ energy decreases, goes below $-U_1$ and approaches the characteristic value $-U_1 - 0.25R_y^*$. Energy of $2p$ state can have minimum. In our case there is no minimum for $2p$ or it is not visible in this scale. Such specific behavior is consequence of competition of two factors: the spatial confinement which increases the energy and presence of the effective potential well that decrease the energy.

In Fig. 3 the binding energy of the hydrogenic impurity is presented as a function of the CdTe/ZnTe dot radius. As shown in this figure, the binding energies increase until they reach the maximum value and then decrease till they become approximately constant at large radii. This behavior is consequence of the shape of $Z = 1$ energies curves. When ($Z = 1$) solution appears, radius and QD

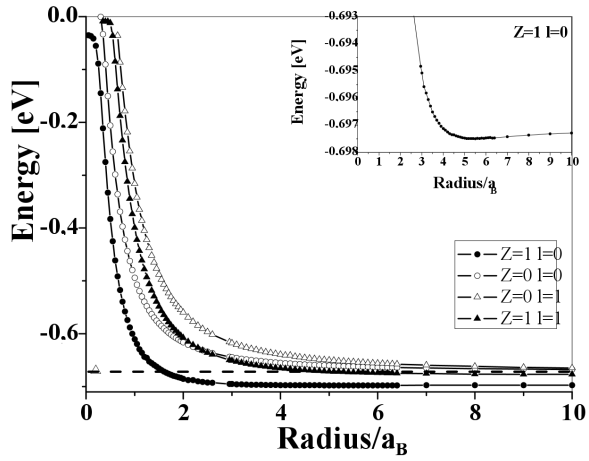

Fig. 2. Energy levels of ground states and first excited states as a function of a dot radii.

volume is small, wave function spreads to the surrounding medium. In hydrogenic impurity presence, when radius increases (QD volume increases) energy of state decreases rapidly. This goes until energy of state reaches approximately $-U_1$. For states below $-U_1$, space where wave function spreads is not dominantly determined by dot dimension but by hydrogenic impurity potential. As a result decrease of energy slow down, get minimum value at characteristic dimension and it starts to increase and asymptotically reaches constant value.

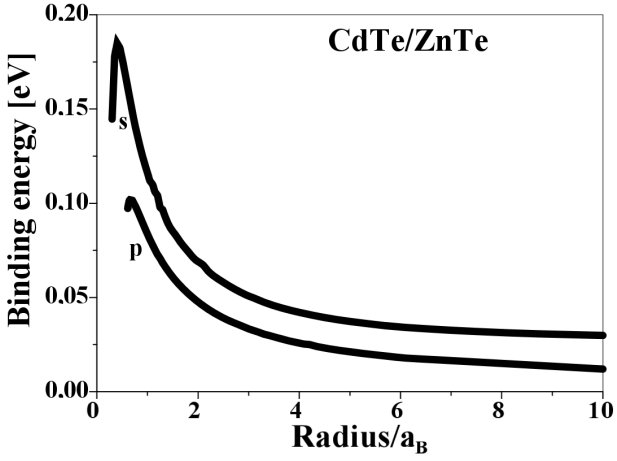

Fig. 3. Binding energy of the D^0 donor impurity as the function of radius r of CdTe/ZnTe spherical QD.

4. Conclusion

In this paper we present D^0 donor in the center of CdTe/ZnTe spherical quantum dot binding energy calculation results. Ground and first excited energy state of D^0 donor are calculated. After introducing Poisson equation solution, i.e. introducing the potential energy

of interaction of ion with an electron in case of different values of the dielectric permittivity of QD (CdTe) and matrix (ZnTe), we exactly solved Schrodinger equation.

Consideration of the exact solution of the Poisson equation allowed us to reveal an important and specific feature of the dependence of the lowest energy states on QD radius. It is the presence of a minimum in the lowest states of D^0 energy spectra.

Acknowledgement

This work is supported by Serbian Ministry of Science, under Projects No. 141047 and No. 141028.

References

[1] D. Bimberg, M. Grundmann, N.N. Lebentsov, *Quantum Dot Heterostructures* (Wiley, Chichester, 1999).

[2] M. Sahin, *Phys. Rev.* **B77**, 045317 (2008).

[3] T. Kazimierczuk, J. Suffczynski, A. Golnik, J.A. Gaj, P. Kossacki, P. Wojnor, *Phys. Rev B* **79**, 153301 (2009).

[4] T. Kazimierczuk, A. Golnik, M. Goryca, P. Wojnor, J.A. Gaj, P. Kossacki, *Acta Phys. Pol. A*, **116**, 882 (2009).

[5] M. Goryca, *Proc. SPIE* Vol. **7600**, 76001N (2010): doi: 10.1117/12.842473.

[6] C-Y. Hsieh, D.S. Chuu, *J. Phys.: Condens. Matter* **12**, 8641 (2000).

[7] M.C. Lin, D.S. Chuu, *J. Appl. Physics* **90**, 2886 (2001).

[8] M.V. Tkach, V.A. Holovatsky, Y.M. Berezovsky, *Phys. Chem. Solid State* **4**, 213 (2003).

[9] V.A. Holovatsky, O.M. Makhanets, O.M. Voitsekhivska, *Physica* E**41**, 1522 (2009).

[10] V.I. Boichuk, I.V. Bilynskyi, R.Ya. Leshko, *Ukr. J. Phys.* **53**, 991 (2008).

[11] M.S. Jang, S.H. Oh, J.C. Choi, H.L. Park, D.C. Choo, M. Jung, D.U. Lee, T.W. Kim, *Solid State Communications* **121**, 571 (2002).

[12] Y. Bae, N. Myung, A. Bard, *Nano Letters* **4**, 1153 (2004).

[13] S. Wang, D. Ding, X. Liu, X.–B. Zhang, D.J. Smith, J.K. Furdyna, Y.–H. Zhang, *J. Cryst. Growth* **311**, 2116 (2009).

[14] N. Tit, I.M. Obaidat, *Physica E* **41**, 23 (2008).

[15] M. Abramowitz, I. Stegun, *Handbook of Mathematical Functions with Formulas, Graphs and Mathematical Tables*, National Bureau of Standards Applied Mathematics Series-55, Nauka, Moskva 1979.